nature medicine

A systems approach identifies HIPK2 as a key regulator of kidney fibrosis

Yuanmeng Jin[1,2,8], Krishna Ratnam[1,8], Peter Y Chuang[1,8], Ying Fan[1], Yifei Zhong[1], Yan Dai[1], Amin R Mazloom[3,4], Edward Y Chen[3,4], Vivette D'Agati[5], Huabao Xiong[6], Michael J Ross[1], Nan Chen[2], Avi Ma'ayan[3,4] & John Cijiang He[1,3,7]

Kidney fibrosis is a common process that leads to the progression of various types of kidney disease. We used an integrated computational and experimental systems biology approach to identify protein kinases that regulate gene expression changes in the kidneys of human immunodeficiency virus (HIV) transgenic mice (Tg26 mice), which have both tubulointerstitial fibrosis and glomerulosclerosis. We identified homeo-domain interacting protein kinase 2 (HIPK2) as a key regulator of kidney fibrosis. HIPK2 was upregulated in the kidneys of Tg26 mice and in those of patients with various kidney diseases. HIV infection increased the protein concentrations of HIPK2 by promoting oxidative stress, which inhibited the seven in absentia homolog 1 (SIAH1)-mediated proteasomal degradation of HIPK2. HIPK2 induced apoptosis and the expression of epithelial-to-mesenchymal transition markers in kidney epithelial cells by activating the p53, transforming growth factor β (TGF-β)–SMAD family member 3 (Smad3) and Wnt-Notch pathways. Knockout of HIPK2 improved renal function and attenuated proteinuria and kidney fibrosis in Tg26 mice, as well as in other murine models of kidney fibrosis. We therefore conclude that HIPK2 is a potential target for anti-fibrosis therapy.

Kidney fibrosis is a final common pathogenic process for many forms of chronic renal disease, including HIV-associated nephropathy (HIVAN), which is a leading cause of renal disease among HIV-infected African Americans[1]. Collapsing focal segmental glomerulosclerosis (FSGS), tubulointerstitial inflammation and fibrosis, tubular dilatation with microcyst formation and renal tubular epithelial cell (RTEC) apoptosis are key pathologic features of HIVAN[2]. HIV directly infects RTECs, but the cellular response to HIV infection is not well defined[3]. An HIV transgenic mouse model (Tg26), which has the proviral transgene pNL4-3: d1443 encoding all the HIV genes except *gag* and *pol*, recapitulates the renal pathologic changes observed in human disease and has been used to study HIVAN pathogenesis[4,5]. Although prior studies have identified individual protein regulators, protein-protein interactions and cell signaling pathways that are altered in HIVAN, a systematic evaluation of these changes has not been attempted.

Transcriptomic measurements are reflective of quantitative changes in mRNA levels but do not provide a direct understanding of the upstream regulatory mechanisms that are responsible for observed changes in gene expression. Identifying potential regulatory mechanisms responsible for changes in gene expression under disease conditions could help to reveal disease mechanisms and enable the discovery of drug targets. Here we present an integrative experimental and computational approach for identifying and ranking protein kinases that are probably responsible for the observed changes in mRNA expression and transcription-factor activation. We computationally predicted that HIPK2 is crucially involved in HIVAN.

HIPK2 is a conserved serine/threonine nuclear kinase that regulates gene expression by phosphorylating transcription factors and accessory components of the transcriptional machinery[6]. HIPK2 is activated in response to morphogenic signals that regulate cell differentiation and apoptosis in neurons[7]. In response to DNA-damaging agents, HIPK2 promotes apoptosis by phosphorylating and activating p53 (ref. 8). HIPK2 also mediates the activation of Wnt[9], Notch[10] and TGF-β–induced signaling[11,12]. Because p53 and TGF-β are known mediators of apoptosis for RTECs[13–15] and the TGF-β, Notch and Wnt–β-catenin pathways promote renal fibrosis[16–19], we hypothesized and experimentally validated that HIPK2, a previously unrecognized kinase in the context of kidney disease, contributes to kidney epithelial cell injury and renal fibrosis in HIVAN and other animal models of renal tubular injury.

RESULTS

HIPK2 is a potential mediator of HIVAN pathogenesis

We confirmed the renal histopathology (**Supplementary Table 1**) and determined genes differentially expressed in the kidney cortices

[1]Division of Nephrology, Department of Medicine, Mount Sinai School of Medicine, New York, New York, USA. [2]Department of Nephrology, Ruijin Hospital, Jiao Tong University School of Medicine, Shanghai, China. [3]Department of Pharmacology and Systems Therapeutics, Mount Sinai School of Medicine, New York, New York, USA. [4]Systems Biology Center New York (SBCNY), New York, New York, USA. [5]Department of Pathology, Columbia University, New York, New York, USA. [6]Immunobiology Center, Mount Sinai School of Medicine, New York, New York, USA. [7]James J. Peters Veteran Administration Medical Center, New York, New York, USA. [8]These authors contributed equally to this work. Correspondence should be addressed to J.C.H. (cijiang.he@mssm.edu) or A.M. (avi.maayan@mssm.edu).

Received 18 October 2011; accepted 23 January 2012; published online 11 March 2012; doi:10.1038/nm.2685

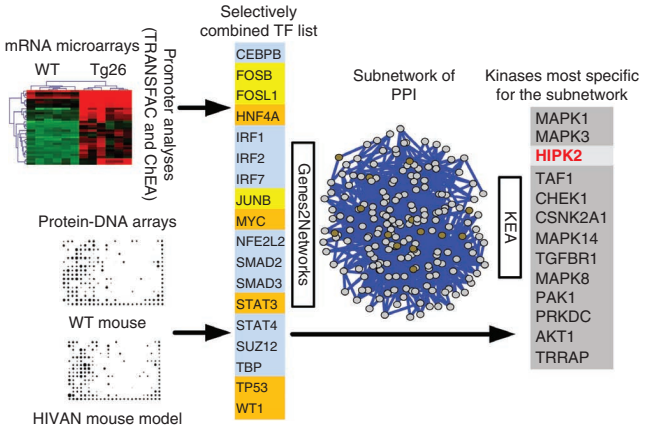

Figure 1 Identification of key signaling pathways activated in HIVAN. Two methods of computational promoter analysis (TRANSFAC and ChEA) and a protein-DNA interaction array were used to identify 18 transcription factors (TFs) differentially activated in kidneys of Tg26 mice. The top five ranked transcription factors from each of the promoter analyses are shown in blue; transcription factors that are in common between TRANSFAC and the protein-DNA interaction array are shown in yellow; and transcription factors that are in common between ChEA and the protein-DNA interaction array are shown in orange. We generated a subnetwork of proteins that interacted with this selectively combined list of 18 transcription factors using Genes2Networks. Proteins within the subnetwork ($n = 205$) were used as inputs for KEA to identify protein kinases that are probably responsible for the phosphorylation of proteins within the subnetwork. HIPK2 is the third most highly ranked kinase (shown in red). PPI, protein-protein interaction.

of Tg26 mice compared to matched wild-type (WT) littermates; 434 genes were significantly upregulated and 72 genes were significantly downregulated in Tg26 mice compared to WT mice (*t* test with false discovery rate $P < 0.01$). We computationally deduced the upstream transcription factors probably responsible for the observed changes in gene expression using two methods. First, we used TRANSFAC matrices[20] to scan the promoter region of genes to identify transcription factors with overrepresented binding sites among the 434 upregulated genes. Using this approach, we identified nine transcription factors (**Supplementary Data**). However, we identified only one transcription factor when we applied the same approach to the 72 downregulated genes. Thus, we used only the upregulated genes in our subsequent analyses. We used a second computational approach (chromatin immunoprecipitation (ChIP) Enrichment Analysis (ChEA)[21]) to identify upstream transcription factors and found a total of 62 (**Supplementary Data**). We experimentally profiled protein-DNA interactions that were differentially regulated between Tg26 and WT kidneys using a protein-DNA binding array (**Fig. 1** and **Supplementary Fig. 1a**). We identified 12 upregulated and 14 downregulated binding interactions for 35 transcription factors (**Supplementary Table 2** and **Supplementary Data**). Some consensus binding motifs on the protein-DNA array were linked to several transcription factors. We confirmed the activity of the selected transcription factors by electrophoretic mobility shift assay (**Supplementary Fig. 1b**). We generated a list of selectively combined transcription factors by including the top five transcription factors from the TRANSFAC analysis and the top five transcription factors from ChEA, as well as transcription factors that were predicted by either TRANSFAC or ChEA and also identified by the protein-DNA interaction array—three for TRANSFAC with the protein-DNA interaction array and five for ChEA with the protein-DNA interaction array—without any overlapping (**Fig. 1** and **Supplementary Data**). These 18 transcription factors are potentially responsible for the pattern of gene expression in the Tg26 kidney.

We linked these transcription factors to upstream regulatory mechanisms by constructing a protein-protein interaction subnetwork based on known interactions (Genes2Networks)[22]. This subnetwork has 205 nodes and was enriched in co-regulators and other transcription factors that physically interact with the 18 transcription factors identified above (**Fig. 1** and **Supplementary Data**). We further linked protein kinases that probably phosphorylate proteins within the subnetwork using Kinase Enrichment Analysis (KEA)[23]. Consistent with our previous studies[24], mitogen-activated protein kinase 3 (MAPK3) and MAPK1 (the canonical MAP kinases ERK1 and ERK2) were highly ranked, whereas the lesser-known kinase HIPK2 was third on the list (**Fig. 1**). HIPK2 has 14 substrates within the subnetwork, which is almost half of all the known substrates for HIPK2 ($n = 34$ total substrates, $P = 2.2 \times 10^{-9}$; **Supplementary Data**).

HIV promotes HIPK2 expression in kidney cells

We examined the expression of HIPK2 in Tg26 kidneys. Immunostaining of HIPK2 revealed that its expression was higher mostly in the tubular compartment and only mildly in glomeruli of Tg26 mice compared to WT mice (**Fig. 2a**). This was confirmed by a western blot analysis of protein lysates from the renal cortex, which contains mostly tubules, and of isolated glomeruli (**Fig. 2b**). The expression of *HIPK2* mRNA in the renal cortex and in isolated glomeruli was not statistically different between Tg26 and WT mice (**Fig. 2c**), suggesting that HIPK2 protein expression was regulated at the posttranslational level. We observed a corresponding higher amount of HIPK2 kinase activity in Tg26 kidneys than WT kidneys (**Fig. 2d**). The amount of HIPK1 and HIPK3 was not different between Tg26 and WT kidneys (data not shown).

To examine whether HIV infection of kidney cells was responsible for the induction of HIPK2 activity, we infected primary human renal tubular epithelial cells (hRTECs) with pseudotyped HIV virions that contained the HIV *gag/pol*-deleted pNL4-3:d1443 proviral DNA. HIPK2 protein expression increased but mRNA levels were unchanged in these cells after infection with HIV (**Fig. 2e**,**f**). HIPK2 kinase activity was increased by HIV infection, and expression of a kinase-dead mutant of HIPK2 (KD-HIPK2) in HIV-infected cells suppressed any HIV-induced increase in HIPK2 kinase activity (**Fig. 2g**). To examine the post-translational regulation of HIPK2 by proteasomal degradation, we treated cells with MG132, which is a specific 26S proteosome inhibitor, and found that HIPK2 expression was significantly increased as a result of this treatment (**Fig. 2h**), which suggests that HIV infection increased HIPK2 activity by reducing HIPK2 proteasomal degradation.

SIAH1 is an upstream regulator of HIPK2

Next, we determined how HIV upregulates HIPK2 protein concentrations. DNA damage increases HIPK2 protein concentrations by inhibiting the ubiquitin ligase SIAH1, which facilitates HIPK2 polyubiquitination and proteasomal degradation[25]. HIV infection promotes oxidative stress[26] and DNA damage[27] in kidney cells. As *SIAH1* expression was reduced in our gene expression microarray data from the Tg26 renal cortex, we sought to examine whether HIV-induced upregulation of HIPK2 was a result of a reduction in SIAH1 concentrations.

We first confirmed that *SIAH1* expression was diminished in the Tg26 renal cortex using real-time PCR (**Fig. 3a**) and western

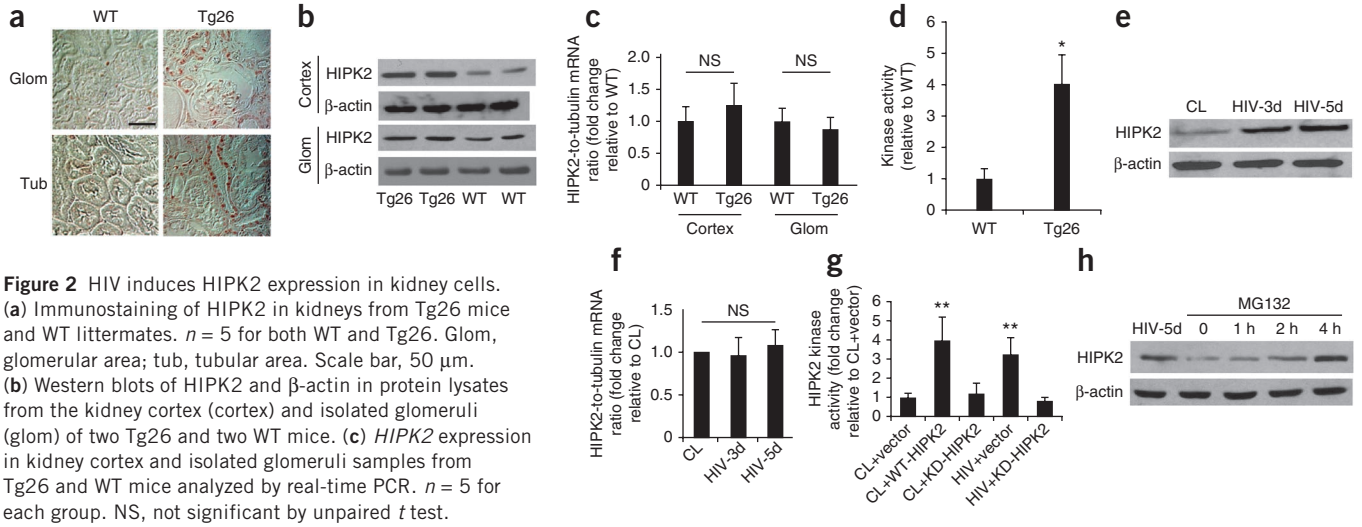

Figure 2 HIV induces HIPK2 expression in kidney cells. (**a**) Immunostaining of HIPK2 in kidneys from Tg26 mice and WT littermates. $n = 5$ for both WT and Tg26. Glom, glomerular area; tub, tubular area. Scale bar, 50 μm. (**b**) Western blots of HIPK2 and β-actin in protein lysates from the kidney cortex (cortex) and isolated glomeruli (glom) of two Tg26 and two WT mice. (**c**) *HIPK2* expression in kidney cortex and isolated glomeruli samples from Tg26 and WT mice analyzed by real-time PCR. $n = 5$ for each group. NS, not significant by unpaired *t* test. (**d**) HIPK2 kinase activity in kidneys of Tg26 and WT mice. $n = 5$. $^*P < 0.001$ by unpaired *t* test. (**e**,**f**) Western blots (**e**) and real-time PCR (**f**) for HIPK2 in hRTECs infected with a control virus (CL) or a pseudotyped HIV-1 virus (HIV) for 3 or 5 d (HIV-3d and HIV-5d, respectively). $n = 4$ for each group. (**g**) HIPK2 kinase activity in hRTECs infected with either control virus or HIV and transfected with an empty expression vector (vector), a WT-HIPK2 vector or a KD-HIPK2 vector. $n = 4$ for each group. $^{**}P < 0.01$ compared to CL+vector by one-way analysis of variance (ANOVA) with Bonferroni's multiple comparison test. (**h**) Western blot of HIPK2 for hRTECs infected with HIV for 5 d or treated with MG132 for the indicated times. Representative blots of three independent experiments are shown for all western blots. Error bars, s.d.

blot (**Fig. 3b**). We observed an inverse relationship between the protein concentrations of SIAH1 and HIPK2 by western blot (**Fig. 3b**) and by immunostaining in adjacent kidney sections (**Fig. 3c**). The weak background staining seen in **Figure 3c** is likely a result of the short development of the stain. Next, we determined whether HIV infection reduces SIAH1 expression. We found that infection of hRTECs by HIV suppressed SIAH1 protein and *SIAH1* mRNA expression (**Fig. 3d**,**e**). To confirm the role of SIAH1 in the regulation of HIPK2, we either overexpressed or silenced *SIAH1* in hRTECs by transfecting a *SIAH1* expression construct or a specific siRNA, respectively (see **Supplementary Fig. 1c**–**e** for the efficiency of the transfections). HIPK2 protein concentration was increased by *SIAH1* knockdown and was reduced by *SIAH1* overexpression (**Fig. 3f**), indicating that SIAH1 acts upstream of HIPK2. To determine the mechanisms by which HIV infection suppressed SIAH1 expression, we treated hRTECs with H_2O_2 and adriamycin and found that both treatments reduced SIAH1 and increased HIPK2 expression (**Fig. 3g**,**h**). Pretreatment with an oxidant scavenger, N-acetylcysteine (NAC), abrogated HIV-induced HIPK2 upregulation and restored SIAH1 expression in the hRTECs (**Fig. 3i**). Treatment with either H_2O_2 or adriamycin did not affect the level of *HIPK2* mRNA in the hRTECs (data not shown).

Expression of SIAH1 and HIPK2 in human kidneys

We corroborated the *in vitro* findings by examining the renal expression of SIAH1 and HIPK2 in different kidney diseases. HIPK2 nuclear staining was markedly higher in kidneys of patients with HIVAN, FSGS, diabetic nephropathy and severe IgA nephropathy (IgAN) compared to kidneys from patients with minimal change disease (MCD) and normal kidneys ($n = 5$ per group for each of the six groups) (**Fig. 3j**). However, we found that HIPK2 staining in kidneys with MCD was not different from that in normal kidneys. Consistent with these findings, tubulointerstitial injury or fibrosis and glomerulosclerosis were present in HIVAN, FSGS, diabetic nephropathy and IgAN kidneys but not MCD kidneys. In both early and late stage HIVAN kidneys, HIPK2 staining in the tubulointerstitial and glomerular areas was higher than the staining of those areas in normal kidneys, but we saw less HIPK2 staining in the glomerular area compared to the tubulointerstitial area of the HIVAN kidneys. Glomerular HIPK2 expression was significantly higher in diabetic nephropathy and IgAN kidneys compared to HIVAN kidneys. HIPK2 staining in FSGS kidneys was higher than normal kidneys and was focal in its distribution.

SIAH1 staining was lower in the tubules of diseased kidneys than in those of normal kidneys and was inversely related to the intensity of HIPK2 staining in all groups (**Fig. 3j**). This inverse relationship between HIPK2 staining and SIAH1 staining was clear in the tubular areas but not in the glomerular areas of FSGS and HIVAN kidneys. In late stage HIVAN glomeruli, HIPK2 staining was lower compared to early stage HIVAN glomeruli, but SIAH1 staining was similar between late and early stage HIVAN glomeruli, suggesting that HIPK2 may be regulated by mechanisms that are independent of SIAH1 in late stage HIVAN glomeruli. A semi-quantitative scoring of the immunostaining data is summarized in **Supplementary Table 3**.

HIPK2 mediates apoptosis and expression of EMT markers

Because RTEC apoptosis is a hallmark of tubulointerstitial injury in HIVAN and HIPK2 is known to mediate apoptosis, we sought to determine the role of HIPK2 in the HIV-induced apoptosis of RTECs. Overexpression of KD-HIPK2 in hRTECs significantly attenuated HIV-induced apoptosis (**Fig. 4a**). In addition, KD-HIPK2 overexpression or siRNA-mediated knockdown of HIPK2 abrogated HIV-induced caspase 3 activity (**Fig. 4b**).

As HIPK2 interacts with the TGF-β pathway, a well known mediator of the epithelial-to-mesenchymal transition (EMT) for RTECs *in vitro* and kidney fibrosis *in vivo*, we examined the effects of HIPK2 on the expression of EMT markers in hRTECs. We found that WT-HIPK2 overexpression or treatment with TGF-β induced the expression of EMT markers, but it not have this effect in cells not overexpressing WT-HIPK2 or in cells treated with TGF-β (**Fig. 4c**). Overexpression of KD-HIPK2 diminished the expression of EMT markers in cells infected with HIV or treated with TGF-β compared to cells not overexpressing KD-HIPK2 (**Fig. 4c**). EMT is characterized

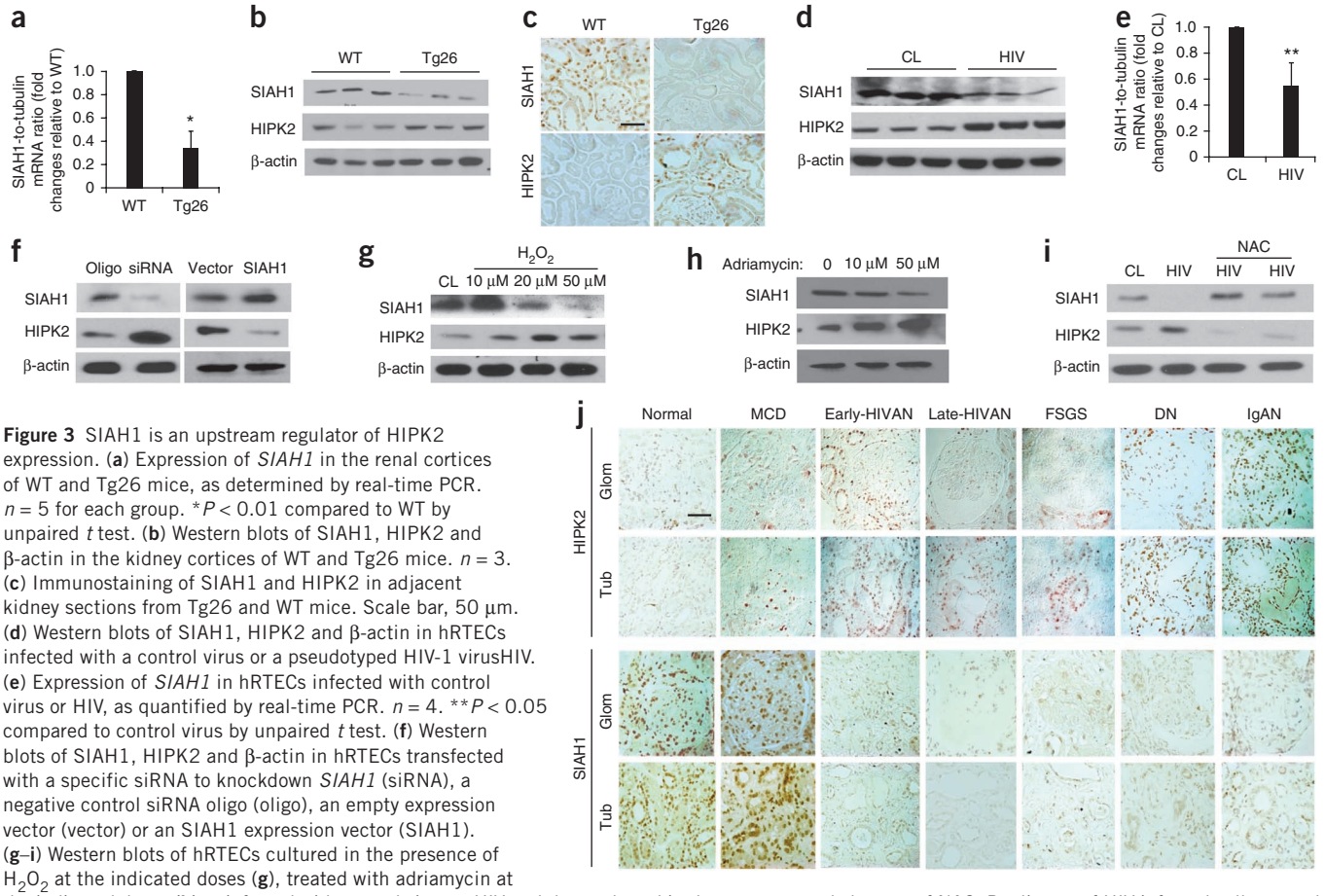

Figure 3 SIAH1 is an upstream regulator of HIPK2 expression. (**a**) Expression of *SIAH1* in the renal cortices of WT and Tg26 mice, as determined by real-time PCR. $n = 5$ for each group. $^{*}P < 0.01$ compared to WT by unpaired *t* test. (**b**) Western blots of SIAH1, HIPK2 and β-actin in the kidney cortices of WT and Tg26 mice. $n = 3$. (**c**) Immunostaining of SIAH1 and HIPK2 in adjacent kidney sections from Tg26 and WT mice. Scale bar, 50 μm. (**d**) Western blots of SIAH1, HIPK2 and β-actin in hRTECs infected with a control virus or a pseudotyped HIV-1 virusHIV. (**e**) Expression of *SIAH1* in hRTECs infected with control virus or HIV, as quantified by real-time PCR. $n = 4$. $^{**}P < 0.05$ compared to control virus by unpaired *t* test. (**f**) Western blots of SIAH1, HIPK2 and β-actin in hRTECs transfected with a specific siRNA to knockdown *SIAH1* (siRNA), a negative control siRNA oligo (oligo), an empty expression vector (vector) or an SIAH1 expression vector (SIAH1). (**g**–**i**) Western blots of hRTECs cultured in the presence of H_2O_2 at the indicated doses (**g**), treated with adriamycin at the indicated doses (**h**) or infected with control virus or HIV and then cultured in the presence and absence of NAC. Replicates of HIV-infected cells treated with NAC are shown (**i**). (**j**) Immunostaining of HIPK2 and SIAH1 in patients with MCD, early stage HIVAN (early-HIVAN), late stage HIVAN (late-HIVAN), FSGS, diabetic nephropathy (DN) or IgAN, and immunostaining of normal nephrectomy samples (normal). Representative fields of glomeruli and tubules are shown. Scale bar, 50 μm. A semi-quantitative scoring of the staining results is summarized in **Supplementary Table 3**. Error bars, s.d.

by gain of α-smooth muscle actin (α–SMA), fibroblast-specific protein 1 (FSP1), and vimentin and loss of E-cadherin. In addition, suppression of HIPK2 activity by either KD-HIPK2 overexpression or siRNA-mediated knockdown prevented TGF-β–induced expression of EMT markers (**Fig. 4c**). Overexpression of KD-HIPK2 restored the expression of E-cadherin in hRTECs treated with TGF-β or infected with HIV (**Fig. 4d**). hRTECs have reduced amounts of E-cadherin when expressing an mCherry–WT-HIPK2 fusion gene and are protected from TGF-β–induced loss of E-cadherin when expressing an mCherry–KD-HIPK2 fusion gene (**Fig. 4d**). We further confirmed the effects of HIPK2 on the expression of EMT markers using western blot (**Fig. 4e**,**f**). We also isolated primary RTECs from HIPK2 knockout (KO) mice and WT littermates. HIV infection induced the expression of EMT markers in WT but not KO RTECs (**Fig. 4g**,**h**).

Role of HIPK2 mediated downstream signaling pathways in hRTECs

Signaling through p53 and TGF-β are known mediators of RTEC apoptosis[13–15]. We found that signaling components of the p53 and TGF-β pathways were among the 14 HIPK2 substrates that were enriched in our subnetwork of protein-protein interactions. Therefore, we sought to determine whether HIPK2 mediated HIV-induced activation of these pathways in hRTECs. For these studies, we used an immortalized proximal tubular epithelial cell line, HK2, because of the limited availability of primary hRTECs and the large number of cells required for these experiments. First, we confirmed that HIPK2 mediated the HIV-induced expression of EMT markers in HK2 cells (**Supplementary Fig. 2a**). We found that KD-HIPK2 inhibited TGF-β–induced phosphorylation of Smad3 (**Fig. 5a**), suggesting that HIPK2 is required for TGF-β–induced Smad3 phosphorylation. We confirmed the interaction of HIPK2 and Smad3 using co-immunoprecipitation (**Supplementary Fig. 2b**). Smad3 phosphorylation was enhanced by HIV infection, but this effect was abrogated by KD-HIPK2 overexpression (**Fig. 5b**). HIV infection also induced p53 phosphorylation in hRTECs, which was blocked by overexpression of KD-HIPK2 (**Fig. 5c**). In addition, we found that HIV infection induced the expression of known target genes of the Wnt–β-catenin and Notch pathways, which was then blocked by overexpression of KD-HIPK2 (**Fig. 5d**,**e**).

HIPK2 is known to upregulate Wnt-mediated transcription by phosphorylating transcription factor 3 (TCF3), a transcriptional repressor, but to inhibit Wnt-mediated transcription by phosphorylating lymphoid enhancer-binding factor 1 (LEF1), a transcriptional activator[28]. Consistent with this, we found that WT-HIPK2 overexpression increased TCF3 phosphorylation, but not LEF1 phosphorylation, in hRTECs (**Supplementary Fig. 2c**). These results show that HIPK2 mediates the HIV-induced activation of the p53, TGF-β and Wnt-Notch pathways in RTECs.

To identify additional downstream HIPK2-mediated signaling pathways, we profiled the protein-DNA interactions and patterns of

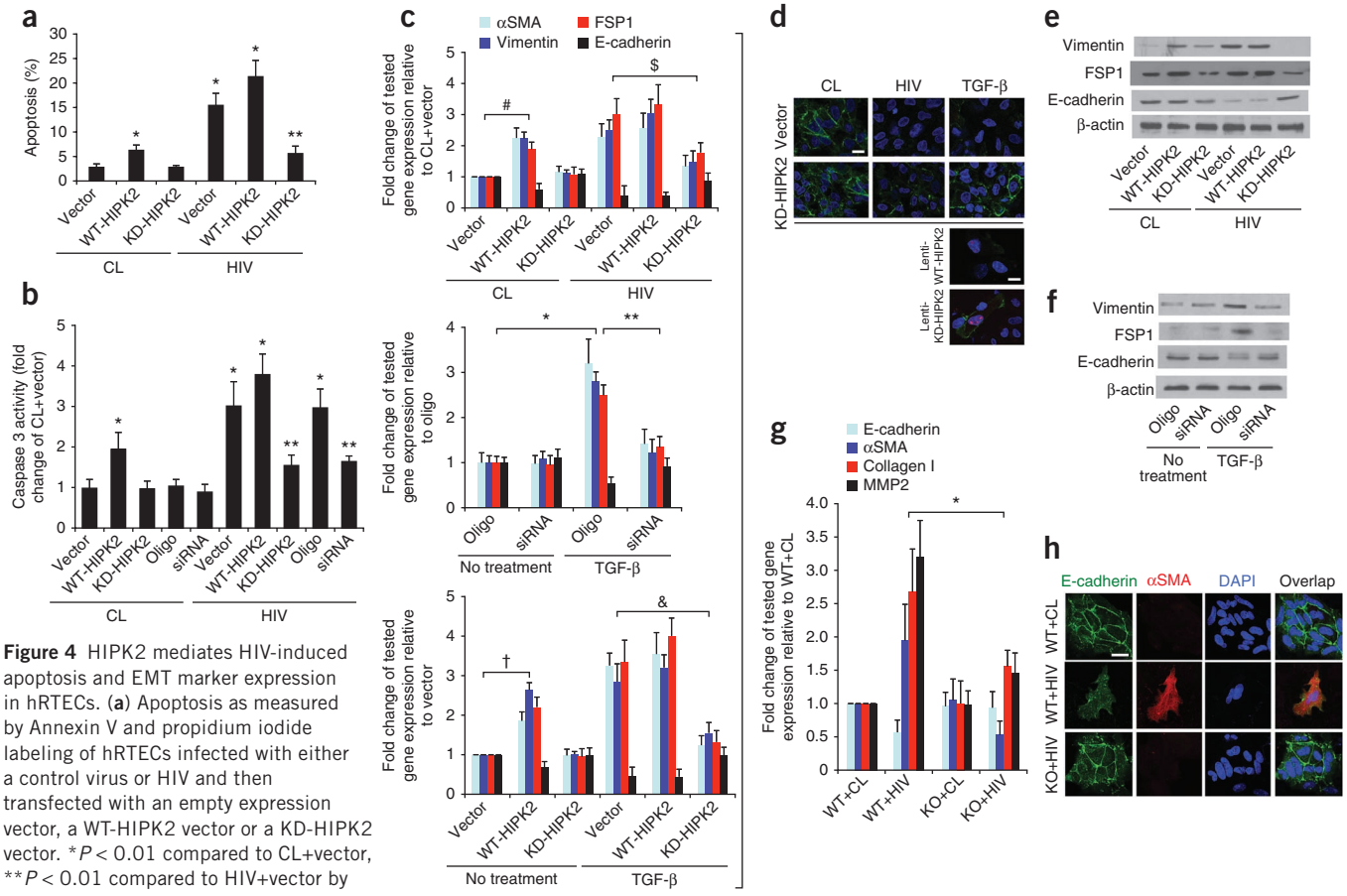

Figure 4 HIPK2 mediates HIV-induced apoptosis and EMT marker expression in hRTECs. (**a**) Apoptosis as measured by Annexin V and propidium iodide labeling of hRTECs infected with either a control virus or HIV and then transfected with an empty expression vector, a WT-HIPK2 vector or a KD-HIPK2 vector. $^{*}P < 0.01$ compared to CL+vector, $^{**}P < 0.01$ compared to HIV+vector by Tukey test after one-way ANOVA. (**b**) Caspase 3 activity of hRTECs infected with control virus or HIV and transfected with vector, WT-HIPK2, KD-HIPK2, a negative control siRNA (oligo) or a specific siRNA to knockdown HIPK2 (siRNA). $n = 4$ for all groups. $^{*}P < 0.01$ compared to CL+vector, $^{**}P < 0.01$ compared to HIV+vector by Tukey test after one-way ANOVA. (**c**, top) Expression of EMT markers in hRTECs infected with HIV or control virus and transfected with vector, WT-HIPK2 or KD-HIPK2. Shown is the fold change in expression relative to the CL+vector group. $n = 4$ for all groups. $^{\#}P < 0.01$ for CL+vector compared to CL+WT-HIPK2, $^{\$}P < 0.05$ for HIV+vector compared to HIV+KD-HIPK2 by Bonferroni test after one-way ANOVA. (**c**, middle) Gene expression of hRTECs transfected with oligo or siRNA and then treated with or without TGF-β. $n = 4$ for all groups. $^{*}P < 0.01$ for oligo compared to oligo+TGF-β, $^{**}P < 0.05$ for oligo+TGF-β compared to siRNA+TGF-β by Bonferroni test after one-way ANOVA. (**c**, bottom) Gene expression in hRTECs transfected with WT-HIPK2, KD-HIPK2 or vector and then incubated with or without TGF-β. $n = 4$ for all groups. $^{\dagger}P < 0.01$ for vector compared to WT-HIPK2, $^{\&}P < 0.05$ for TGF-β+vector compared to TGF-β+KD-HIPK2 by Bonferroni test after one-way ANOVA. (**d**, top two rows) Immunofluorescent staining of E-cadherin in hRTECs transfected with vector or KD-HIPK2 and then infected with either control virus or HIV or treated with TGF-β. (**d**, bottom two rows) Immunostaining of E-cadherin in hRTECs transduced with lentivectors to overexpress a fusion protein of mCherry with WT-HIPK2 (lenti–WT-HIPK2) or KD-HIPK2 (lenti–KD-HIPK2) and treated with TGF-β. E-cadherin is shown in green, nuclear staining with DAPI is shown in blue, and mCherry fusion proteins are shown in magenta. Representative results of three experiments are shown. Scale bars, 10 μm. (**e**,**f**) Western blots of hRTECs cultured in the same condition as in the upper graph of **c** (**e**) and as in the middle graph of **c** (**f**). Representative blots of three independent experiments are shown. (**g**) Expression of targeted genes in primary renal tubular cells isolated from HIPK2 KO mice and their WT littermates infected with control virus or HIV and then quantified by real-time PCR. $n = 4$ for all groups. $^{*}P < 0.01$ for WT+HIV compared to KO+HIV. MMP2, matrix metallopeptidase 2. (**h**) Immunofluorescent staining of E-cadherin, αSMA and DAPI in primary RTECs isolated from WT mice and infected with control virus or HIV or from KO mice infected with HIV. Scale bar, 10 μm. Error bars, s.d.

gene expression in human embryonic kidney cells with HIPK2 overexpression (HEK293 cells). We chose the human embryonic kidney cell line for its high efficiency of transfection. Fourteen transcription factors were upregulated and 15 transcription factors were downregulated by HIPK2 overexpression in the protein-DNA interaction arrays (**Supplementary Table 4**). Of the upregulated interactions, nuclear factor-κB (NF-κB) and signal transducer and activator of transcription 3 (Stat3) are known to be activated in the Tg26 kidney. We also identified p53 and a downstream nuclear mediator of the TGF-β pathway, Smad3, as upregulated transcription factors. Furthermore, Snail[29] and v-ets erythroblastosis virus E26 oncogene homolog 1 (Ets1)[30]—two transcription factors known to mediate kidney fibrosis—were also upregulated. A promoter analysis of differentially expressed genes in the microarrays identified an enrichment of NF-κB and Stat3 target genes (**Supplementary Table 5**). To confirm that NF-κB is a key transcription factor downstream of HIPK2, we examined NF-κB activation using a luciferase reporter assay. In hRTECs, KD-HIPK2 overexpression suppressed tumor necrosis factor α (TNF-α)–induced activation of NF-κB (treatment with TNF-α compared to no treatment, 10.32 ± 1.22 fold increase in relative luminescence unit (mean ± s.d.); treatment with TNF-α and KD-HIPK2 overexpression compared to no treatment and KD-HIPK2 overexpression, 2.41 ± 0.65 fold change in relative luminescence unit; $n = 4$ for all groups; $P < 0.01$ for TNF-α–treated cells compared to cells treated with TNF-α and KD-HIPK2 overexpression). We also confirmed that KD-HIPK2 overexpression inhibited, whereas

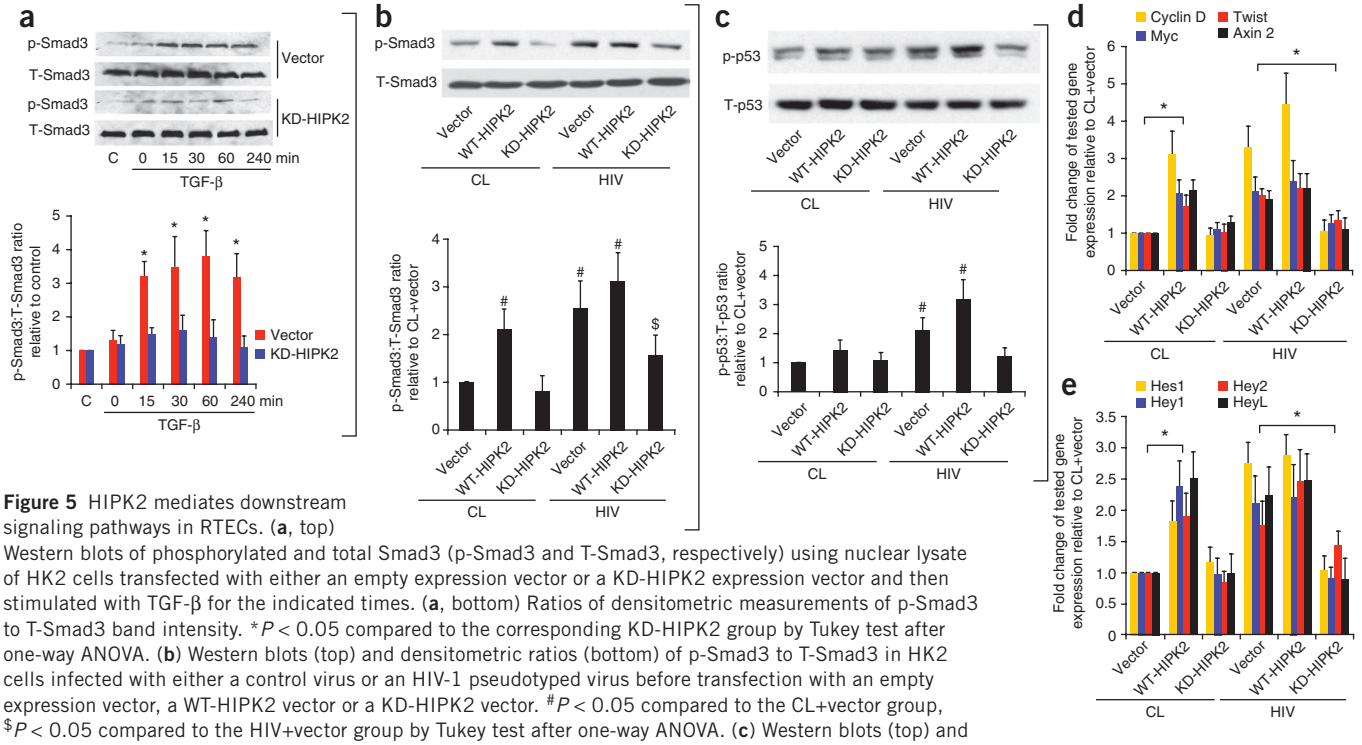

Figure 5 HIPK2 mediates downstream signaling pathways in RTECs. (**a**, top) Western blots of phosphorylated and total Smad3 (p-Smad3 and T-Smad3, respectively) using nuclear lysate of HK2 cells transfected with either an empty expression vector or a KD-HIPK2 expression vector and then stimulated with TGF-β for the indicated times. (**a**, bottom) Ratios of densitometric measurements of p-Smad3 to T-Smad3 band intensity. $^{*}P < 0.05$ compared to the corresponding KD-HIPK2 group by Tukey test after one-way ANOVA. (**b**) Western blots (top) and densitometric ratios (bottom) of p-Smad3 to T-Smad3 in HK2 cells infected with either a control virus or an HIV-1 pseudotyped virus before transfection with an empty expression vector, a WT-HIPK2 vector or a KD-HIPK2 vector. $^{\#}P < 0.05$ compared to the CL+vector group, $^{\$}P < 0.05$ compared to the HIV+vector group by Tukey test after one-way ANOVA. (**c**) Western blots (top) and densitometric ratios (bottom) of phosphorylated p53 (p-p53) to total p53 (T-p53) in primary hRTECs. $^{\#}P < 0.05$ compared to the CL+vector group by Tukey test after one-way ANOVA. (**d**,**e**) Expression of genes involved in the Wnt–β-catenin (**d**) and Notch (**e**) signaling pathways from primary hRTECs. $^{*}P < 0.05$ for all tested genes between the indicated groups by Tukey test after one-way ANOVA. Representative blots are shown. Myc, myelocytomatosis oncogene; Hes1, hairy and enhancer of split 1; Hey1, hairy/enhancer-of-split related with YRPW motif 1; HeyL, hairy/enhancer-of-split related with YRPW motif-like. Error bars, s.d.

WT-HIPK2 overexpression induced, the expression of NF-κB–targeted genes in HIV-infected hRTECs (**Supplementary Fig. 2d**). A pathway analysis of genes upregulated by HIPK2 using WikiPathways[31] showed that the TGF-β–receptor and Wnt-signaling pathways were both highly ranked (**Supplementary Table 5**). These unbiased analyses confirmed that the TGF-β–Smad3, Wnt, p53 and NF-κB pathways are key pathways downstream of HIPK2.

Knockout of HIPK2 attenuates kidney fibrosis in Tg26 mice

We identified HIPK2 as a key regulator of RTEC apoptosis and expression of EMT markers *in vitro*. However, debate exists within the field as to whether the EMT of RTECs *in vitro* correlates with renal fibrosis *in vivo*[32]. To verify the *in vivo* role of HIPK2, we generated knockout-transgenic hybrid mice that were knocked out for HIPK2 and expressed the HIV transgene (KO-Tg26 mice). KO mice have no obvious renal phenotype[33,34]. Tg26 mice typically develop proteinuria starting at 4 weeks of age. KO-Tg26 mice had lower amounts of proteinuria compared to Tg26 mice (**Fig. 6a**). KO-Tg26 mice had lower concentrations of serum urea nitrogen, which is a marker of renal function, compared to Tg26 mice (**Fig. 6b**). Tubulointerstitial injury and fibrosis were also significantly attenuated in KO-Tg26 mice compared to Tg26 mice (**Fig. 6c**,**d** and **Supplementary Table 6**). We confirmed the reduction in renal fibrosis in KO-Tg26 mice by measurements of the collagen content within the renal cortices of the mice (**Fig. 6e**). Podocyte hyperplasia and glomerulosclerosis were also lower in KO-Tg26 compared to Tg26 mice (**Supplementary Table 6**). The expression of EMT markers was significantly higher in the kidney cortices of Tg26 mice, but not KO-Tg26 mice, compared to WT mice (**Fig. 6f**,**g** and **Supplementary Fig. 2e**). The expression of genes targeted by Wnt-Notch (**Fig. 6f**) and NF-κB (**Fig. 6h**) was higher in the kidney cortices of Tg26 compared to KO-Tg26 mice. Phosphorylation of p53, Smad3 and NFkB was also higher in the kidneys of Tg26 compared to KO-Tg26 mice (**Fig. 6g**). We confirmed the greater amount of nuclear staining of β-catenin, which is a marker of EMT[35], and phosphorylated Smad3 in the kidneys of Tg26 compared to KO-Tg26 mice (**Supplementary Fig. 2e**).

Together, these findings show that knockout of *HIPK2* abolished the HIV-induced activation of the p53, TGF-β–Smad3 and Wnt-Notch pathways in the kidney cortices of Tg26 mice. We also confirmed that expression of the HIV *nef* gene was not lower in KO-Tg26 mice than in Tg26 mice (data not shown) to ensure that reduction of HIPK2 expression did not interfere with HIV viral gene expression as a confounding experimental factor.

HIPK2 in HIV-induced podocyte de-differentiation and EMT

As HIPK2 protein expression is higher in the glomeruli of Tg26 mice than WT mice, and as KO-Tg26 mice had lower proteinuria, podocyte hyperplasia, and glomerulosclerosis than Tg26 mice, we sought to determine the role of HIPK2 in HIV-induced podocyte de-differentiation and EMT. Glomerular expression of EMT markers was higher and glomerular expression of podocyte differentiation markers was lower in Tg26 mice, but not KO-Tg26 mice, compared to WT mice (**Supplementary Fig. 3a–c**). The glomerular expression of genes targeted by Wnt-Notch and NF-κB was enhanced in Tg26 mice, but not KO-Tg26 mice, compared to WT mice (**Supplementary Fig. 3d**,**e**). *HIPK2* expression was the same in all groups of mice (**Supplementary Fig. 3d**). Smad3 phosphorylation was greater in Tg26 compared KO-Tg26 glomeruli (**Supplementary Fig. 3f**). We also confirmed that

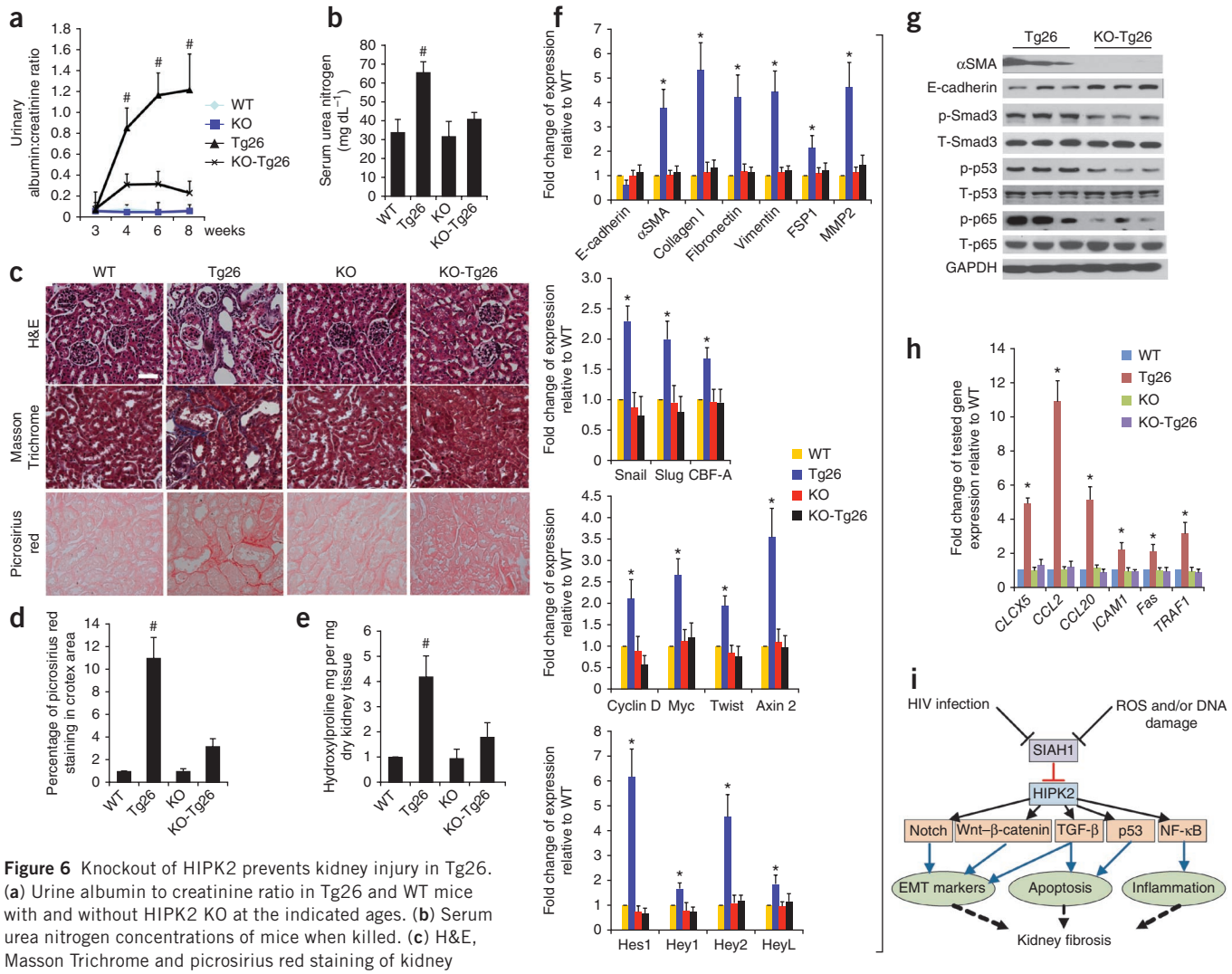

Figure 6 Knockout of HIPK2 prevents kidney injury in Tg26. (**a**) Urine albumin to creatinine ratio in Tg26 and WT mice with and without HIPK2 KO at the indicated ages. (**b**) Serum urea nitrogen concentrations of mice when killed. (**c**) H&E, Masson Trichrome and picrosirius red staining of kidney sections. Representative images of six mice for each group are shown. Scale bar, 50 μm. (**d**) Quantification of the percentage of the area with picrosirius red staining by morphometric analysis. (**e**) Quantification of the hydroxyproline content in kidney tissue. (**f**) Expression of EMT markers (top two graphs in **f**) and target genes of Wnt–β-catenin (third graph in **f**) and Notch (bottom graph in **f**). Slug, Snail homolog 2; CBF-A, CArG box-binding factor-A. (**g**) Western blots for αSMA, E-cadherin, GAPDH and phosphorylated and total Smad3, p53 and p65. Representative blots from three mice in each group are shown. (**h**) Relative mRNA expression of genes targeted by NF-κB signaling. CXCL5, C-X-C motif chemokine 5; CCL2, chemokine C-C motif ligand 2; CCL20, chemokine C-C motif ligand 20; ICAM1, intercellular adhesion molecule 1; Fas, TNF receptor superfamily member 6; TRAF1, TNF receptor-associated factor 1. (**i**) A schematic that summarizes the flow of signals from initial insults (HIV infection or oxidative stress) to the suppression of SIAH1 expression, the expression of HIPK2 and the activation of multiple signaling pathways involved in kidney fibrosis. $^{\#}P < 0.05$ compared to KO-Tg26, $^{*}P < 0.05$ comparing Tg26 against WT, KO and KO-Tg26 by Bonferroni test after ANOVA. $n = 6$ for all groups. Error bars, s.d.

KD-HIPK2 overexpression suppressed the expression of desmin and Snail1, restored the expression of nephrin and the tight junction protein ZO-1, inhibited the HIV-induced expression of Wnt-Notch– and NF-κB–targeted genes and attenuated HIV-induced Smad3 phosphorylation in podocytes (**Supplementary Fig. 3g–j**). These data validated the role of HIPK2 in the HIV-induced activation of profibrotic pathways in podocytes.

Oxidant stress and the expression of SIAH1 and HIPK2

Because our *in vitro* studies showed that inhibition of ROS by NAC restored the expression of SIAH1 and suppressed HIPK2 expression in HIV-infected RTECs, we investigated the cellular effects of NAC treatment on HIV-infected hRTECs. NAC treatment attenuated the HIV-induced increase in caspase 3 activity and EMT-marker expression (**Supplementary Fig. 4a,b**). Treatment of Tg26 mice with NAC partially attenuated the proteinuria, serum urea nitrogen elevation and kidney fibrosis in these mice (**Supplementary Fig. 4c–f**). Using western blot, we confirmed that NAC treatment increased the amount of SIAH1, suppressed the amount of HIPK2 and increased the ratio of reduced to oxidized glutathione in the renal cortices of Tg26 mice compared to those of vehicle-treated Tg26 mice (**Supplementary Fig. 4g,h**). These findings confirmed that reactive oxygen species (ROS) mediate HIV-induced HIPK2 expression and kidney fibrosis in Tg26 mice.

Role of HIPK2 in other models of renal fibrosis

Because our *in vitro* studies suggested that HIPK2 mediates the TGF-β–induced expression of EMT markers in RTECs, we hypothesized that HIPK2 might have a more general role in renal fibrosis. We tested this hypothesis in a well established model of renal fibrosis: unilateral ureteral obstruction (UUO). We found that HIPK2 was higher in

the tubulointerstitium of WT kidneys with UUO compared to the sham-operated WT kidneys, sham-operated KO-HIPK2 kidneys and UUO KO-HIPK2 kidneys (**Supplementary Fig. 5a**). UUO increased fibrosis in WT but not KO-HIPK2 kidneys, as confirmed by both Masson Trichrome and picrosirius red staining (**Supplementary Fig. 5a**). SIAH1 expression was lower and HIPK2 expression was higher in WT-UUO kidneys than WT sham-operated kidneys (**Supplementary Fig. 5b**). We confirmed renal fibrosis using quantification of the morphometric measurements of picrosirius red staining and collagen content in the renal cortices of all four groups of mice (**Supplementary Fig. 5c**). Renal expression of the EMT markers (**Supplementary Fig. 5d**,**e**), as well as nuclear β-catenin and phosphorylated Smad3 staining (**Supplementary Fig. 5f**), were higher in WT-UUO kidneys, but not KO-UUO kidneys, compared to WT sham-operated kidneys. We further confirmed Smad3 phosphorylation in all four groups of mice by western blot analysis (**Supplementary Fig. 5g**). We also examined the expression of Wnt-Notch target genes, which were upregulated in WT-UUO mice, but not KO-UUO mice, compared to WT sham-operated mice (**Supplementary Fig. 5h**). These data indicate that HIPK2 knockout *in vivo* prevents tubulointerstitial fibrosis and the expression of EMT markers in the UUO model.

We also examined the role of HIPK2 in a third model of renal fibrosis: folic-acid–induced renal fibrosis[36–38]. We found that KO-HIPK2 mice are protected from folic-acid–induced kidney fibrosis, as shown by renal histology and measurements of kidney hydroxylproline content (**Supplementary Fig. 6a**,**b**). Serum urea nitrogen concentrations and the renal expression of EMT markers were similarly reduced in KO mice treated with folic acid compared to WT mice treated with folic acid (**Supplementary Fig. 6c**,**d**).

DISCUSSION

In this study, we integrated experimental and computational approaches to identify protein kinases responsible for the observed gene regulation changes in a disease state. Using this approach, we identified MAPK1 (ERK2), MAPK3 (ERK1) and HIPK2 as the top three protein kinases mediating gene expression in the Tg26 kidney. We previously showed that ERK mediates HIV-induced podocyte proliferation and RTEC apoptosis[24,39]. Here, we identified HIPK2 as a key regulator of EMT *in vitro* and kidney fibrosis *in vivo*. Our data suggest that both ERK and HIPK2 are crucial for HIV-induced kidney disease. Further studies will be required to determine what crosstalk takes place between the ERK and HIPK2 pathways.

We confirmed that HIPK2 expression is higher not only in kidneys of Tg26 mice and patients with HIVAN but also in kidneys of patients with FSGS, diabetic nephropathy and IgAN. This supports a more general role for HIPK2 in human kidney diseases, which was corroborated by the fact that HIPK2 mediates renal fibrosis in three established mouse models of renal fibrosis (Tg26, UUO and folic-acid–induced renal fibrosis).

We found that HIPK2 mediates HIV-induced apoptosis and the expression of EMT markers in cultured hRTECs. Apoptosis and EMT of RTECs leading to renal fibrosis have been described in many kidney diseases, including HIVAN[40–43]. Recent studies have suggested that complete EMT of RTECs may not occur *in vivo*. However, RTECs can gain EMT markers (epithelial plasticity in fibrogenesis) after injury[44,45]. Our data suggest that HIPK2 mediates expression of EMT markers in RTECs both *in vitro* and *in vivo*.

Our data indicate that HIPK2 expression is increased in the RTECs as well as in the glomeruli of diseased kidneys. It is possible that fibroblasts, pericytes or both also express HIPK2. We found that HIPK2 mediates the HIV-induced de-differentiation of podocytes and the expression of EMT markers in RTECs. Consistent with this, knockout of HIPK2 markedly reduced proteinuria, podocyte hyperplasia and glomerulosclerosis in Tg26 mice. Future studies will be needed to determine whether HIPK2 is required for the activation of fibroblasts, pericytes or both or whether HIPK2 mediates RTEC-fibroblast crosstalk.

In this study, we focused on the intracellular mechanisms of HIPK2 regulation in diseased kidneys. We found that infection with HIV decreases SIAH1 expression through DNA damage and oxidative stress, leading to the accumulation of HIPK2. In addition, we confirmed that inhibition of ROS by NAC restores SIAH1 expression, reduces HIPK2 protein concentrations and attenuates kidney injury and fibrosis in Tg26 mice. Although the renal protective effects of NAC in human kidney disease remain unresolved[46], our data indicate that anti-ROS therapy could be a potential approach to treat patients with kidney fibrosis. Our findings are consistent with prior studies reporting that polyubiquitination promotes HIPK2 degradation[47] and that DNA damage and oxidative stress activate HIPK2 (ref. 48).

We confirmed that HIPK2 mediates TGF-β–induced and HIV-induced pro-apoptotic and pro-fibrotic pathways in RTECs, including the p53, Smad3 and Notch-Wnt pathways. Previous studies showed that HIPK2 can either repress or promote transcriptional activation mediated by Wnt–β-catenin[9,34]. Consistent with this, recent studies suggested that HIPK2 could affect the Wnt pathway in a context-dependent manner[28]. HIPK2 upregulates Wnt-mediated transcription by phosphorylating TCF3, a transcriptional repressor, but inhibits Wnt-mediated transcription by phosphorylating LEF1, a transcriptional activator[28]. Consistent with this, we found that overexpression of WT-HIPK2 increases TCF3 phosphorylation, but not LEF1 phosphorylation, in RTECs. NF-κB–mediated inflammation is known to cause tissue injury and fibrosis. Our studies also suggest that HIPK2 is a key regulator of the NF-κB pathway, which is a new finding that has not been previously explored, to our knowledge. These findings, summarized in **Figure 6i**, show that signals from initial insults, such as DNA damage or oxidative stress, increase HIPK2 expression to activate multiple signaling pathways that are involved in kidney fibrosis.

In conclusion, we present here a systems approach to identifying upstream protein kinases based on genome-wide mRNA expression microarrays and DNA-protein arrays. We identified and confirmed that HIPK2, a protein kinase previously unrecognized in kidney disease, has a crucial role in renal fibrosis. We elucidated the regulation of HIPK2 in kidney disease and in downstream signaling pathways that mediate HIPK2-induced apoptosis, as well as the expression of EMT markers in kidney cells. We believe that HIPK2 could be a new therapeutic target for kidney disease, especially as protein kinases are 'drugable' targets.

METHODS

Methods and any associated references are available in the online version of the paper at http://www.nature.com/naturemedicine/.

Accession codes. The microarray data has been deposited in Gene Expression Omnibus with the accession code GSE35226 (NCBI tracking system 16249557).

Note: Supplementary information is available on the Nature Medicine website.

ACKNOWLEDGMENTS

The authors acknowledge and thank G.L. Gusella (Mount Sinai School of Medicine, New York) for providing the lentiviral construct, E. Huang (University of California

San Francisco) for providing the HIPK2 KO mice, P. Mundel (Massachusetts General Hospital, Boston) for synaptopodin antibody and conditionally immortalized murine podocyte cell line, L. Holzman (University of Pennsylvania, Philadelphia) for nephrin antibody and R.H. Goodman (Oregon Health and Science University, Portland) for WT-HIPK2 and KD-HIPK2 constructs. We also thank R. Iyengar and P. Klotman for critical suggestions on experimental design and for other valuable contributions. J.C.H. is supported by US National Institutes of Health (NIH) grant 1R01DK078897 and a Veterans Affairs Merit Award; J.C.H. and A.M. are supported by NIH 1R01DK088541, NIH P01-DK-56492 and NIH 1RC4DK090860; A.M. is supported by NIH RC2OD006536 and 5P50GM071558; P.Y.C. is supported by NIH 5K08DK082760. N.C. is supported by Chinese 973 fund 2012CB517601.

AUTHOR CONTRIBUTIONS

J.C.H., A.M., P.Y.C., Y.J., N.C. and K.R. designed the research project; Y.J., K.R., Y.F., Y.Z., M.J.R., H.X. and P.Y.C. performed the experiments; P.Y.C. and Y.D. prepared lentiviral constructs for HIPK2; V.D. analyzed the pathologic findings; A.M., E.Y.C. and A.R.M. performed bioinformatics and systems biology analyses; J.C.H., P.Y.C. and A.M. wrote the manuscript, and all authors contributed to the preparation of the manuscript.

COMPETING FINANCIAL INTERESTS

The authors declare no competing financial interests.

Published online at http://www.nature.com/naturemedicine/.
Reprints and permissions information is available online at http://www.nature.com/reprints/index.html.

1. Wyatt, C.M. & Klotman, P.E. HIV-associated nephropathy in the era of antiretroviral therapy. *Am. J. Med.* **120**, 488–492 (2007).
2. Leventhal, J.S. & Ross, M.J. Pathogenesis of HIV-associated nephropathy. *Semin. Nephrol.* **28**, 523–534 (2008).
3. Bruggeman, L.A. *et al.* Renal epithelium is a previously unrecognized site of HIV-1 infection. *J. Am. Soc. Nephrol.* **11**, 2079–2087 (2000).
4. Kopp, J.B. *et al.* Progressive glomerulosclerosis and enhanced renal accumulation of basement membrane components in mice transgenic for human immunodeficiency virus type 1 genes. *Proc. Natl. Acad. Sci. USA* **89**, 1577–1581 (1992).
5. Dickie, P. *et al.* HIV-associated nephropathy in transgenic mice expressing HIV-1 genes. *Virology* **185**, 109–119 (1991).
6. Calzado, M.A., Renner, F., Roscic, A. & Schmitz, M.L. HIPK2: a versatile switchboard regulating the transcription machinery and cell death. *Cell Cycle* **6**, 139–143 (2007).
7. Isono, K. *et al.* Overlapping roles for homeodomain-interacting protein kinases hipk1 and hipk2 in the mediation of cell growth in response to morphogenetic and genotoxic signals. *Mol. Cell. Biol.* **26**, 2758–2771 (2006).
8. D'Orazi, G. *et al.* Homeodomain-interacting protein kinase-2 phosphorylates p53 at Ser 46 and mediates apoptosis. *Nat. Cell Biol.* **4**, 11–19 (2002).
9. Lee, W., Swarup, S., Chen, J., Ishitani, T. & Verheyen, E.M. Homeodomain-interacting protein kinases (Hipks) promote Wnt/Wg signaling through stabilization of β-catenin/Arm and stimulation of target gene expression. *Development* **136**, 241–251 (2009).
10. Lee, W., Andrews, B.C., Faust, M., Walldorf, U. & Verheyen, E.M. Hipk is an essential protein that promotes Notch signal transduction in the *Drosophila* eye by inhibition of the global co-repressor Groucho. *Dev. Biol.* **325**, 263–272 (2009).
11. Zhang, J. *et al.* Essential function of HIPK2 in TGFβ-dependent survival of midbrain dopamine neurons. *Nat. Neurosci.* **10**, 77–86 (2007).
12. Hofmann, T.G., Stollberg, N., Schmitz, M.L. & Will, H. HIPK2 regulates transforming growth factor-β–induced c-Jun NH(2)-terminal kinase activation and apoptosis in human hepatoma cells. *Cancer Res.* **63**, 8271–8277 (2003).
13. Seth, R., Yang, C., Kaushal, V., Shah, S.V. & Kaushal, G.P. p53-dependent caspase-2 activation in mitochondrial release of apoptosis-inducing factor and its role in renal tubular epithelial cell injury. *J. Biol. Chem.* **280**, 31230–31239 (2005).
14. Yoo, J. *et al.* Transforming growth factor-β–induced apoptosis is mediated by Smad-dependent expression of GADD45b through p38 activation. *J. Biol. Chem.* **278**, 43001–43007 (2003).
15. Inazaki, K. *et al.* Smad3 deficiency attenuates renal fibrosis, inflammation,and apoptosis after unilateral ureteral obstruction. *Kidney Int.* **66**, 597–604 (2004).
16. Zeisberg, M. *et al.* BMP-7 counteracts TGF-β1–induced epithelial-to-mesenchymal transition and reverses chronic renal injury. *Nat. Med.* **9**, 964–968 (2003).
17. Vincent, T. *et al.* A SNAIL1-SMAD3/4 transcriptional repressor complex promotes TGF-β mediated epithelial-mesenchymal transition. *Nat. Cell Biol.* **11**, 943–950 (2009).
18. Zavadil, J., Cermak, L., Soto-Nieves, N. & Bottinger, E.P. Integration of TGF-β/Smad and Jagged1/Notch signalling in epithelial-to-mesenchymal transition. *EMBO J.* **23**, 1155–1165 (2004).
19. Zavadil, J. & Bottinger, E.P. TGF-β and epithelial-to-mesenchymal transitions. *Oncogene* **24**, 5764–5774 (2005).
20. Matys, V. *et al.* TRANSFAC: transcriptional regulation, from patterns to profiles. *Nucleic Acids Res.* **31**, 374–378 (2003).
21. Lachmann, A. *et al.* ChEA: transcription factor regulation inferred from integrating genome-wide ChIP-X experiments. *Bioinformatics* **26**, 2438–2444 (2010).
22. Berger, S.I., Posner, J.M. & Ma'ayan, A. Genes2Networks: connecting lists of gene symbols using mammalian protein interactions databases. *BMC Bioinformatics* **8**, 372 (2007).
23. Lachmann, A. & Ma'ayan, A. KEA: kinase enrichment analysis. *Bioinformatics* **25**, 684–686 (2009).
24. He, J.C. *et al.* Nef stimulates proliferation of glomerular podocytes through activation of Src-dependent Stat3 and MAPK1,2 pathways. *J. Clin. Invest.* **114**, 643–651 (2004).
25. Winter, M. *et al.* Control of HIPK2 stability by ubiquitin ligase Siah-1 and checkpoint kinases ATM and ATR. *Nat. Cell Biol.* **10**, 812–824 (2008).
26. Husain, M. *et al.* Inhibition of p66ShcA longevity gene rescues podocytes from HIV-1–induced oxidative stress and apoptosis. *J. Biol. Chem.* **284**, 16648–16658 (2009).
27. Rosenstiel, P.E. *et al.* HIV-1 Vpr activates the DNA damage response in renal tubule epithelial cells. *AIDS* **23**, 2054–2056 (2009).
28. Hikasa, H. & Sokol, S.Y. Phosphorylation of TCF proteins by homeodomain-interacting protein kinase 2. *J. Biol. Chem.* **286**, 12093–12100 (2011).
29. Boutet, A. *et al.* Snail activation disrupts tissue homeostasis and induces fibrosis in the adult kidney. *EMBO J.* **25**, 5603–5613 (2006).
30. Mizui, M. *et al.* Transcription factor Ets-1 is essential for mesangial matrix remodeling. *Kidney Int.* **70**, 298–305 (2006).
31. Pico, A.R. *et al.* WikiPathways: pathway editing for the people. *PLoS Biol.* **6**, e184 (2008).
32. Kriz, W., Kaissling, B. & Le Hir, M. Epithelial-mesenchymal transition (EMT) in kidney fibrosis: fact or fantasy? *J. Clin. Invest.* **121**, 468–474 (2011).
33. Zhang, Q., Yoshimatsu, Y., Hildebrand, J., Frisch, S.M. & Goodman, R.H. Homeodomain interacting protein kinase 2 promotes apoptosis by downregulating the transcriptional corepressor CtBP. *Cell* **115**, 177–186 (2003).
34. Wei, G. *et al.* HIPK2 represses β-catenin–mediated transcription, epidermal stem cell expansion, and skin tumorigenesis. *Proc. Natl. Acad. Sci. USA* **104**, 13040–13045 (2007).
35. Hertig, A. [Epithelial-mesenchymal transition of the renal graft]. *Nephrol. Ther.* **4** (suppl. 1), S25–S28 (2008).
36. Long, D.A. *et al.* Angiopoietin-1 therapy enhances fibrosis and inflammation following folic acid-induced acute renal injury. *Kidney Int.* **74**, 300–309 (2008).
37. Doi, K. *et al.* Attenuation of folic acid-induced renal inflammatory injury in platelet-activating factor receptor–deficient mice. *Am. J. Pathol.* **168**, 1413–1424 (2006).
38. Bielesz, B. *et al.* Epithelial Notch signaling regulates interstitial fibrosis development in the kidneys of mice and humans. *J. Clin. Invest.* **120**, 4040–4054 (2010).
39. Snyder, A. *et al.* HIV-1 viral protein r induces ERK and caspase-8–dependent apoptosis in renal tubular epithelial cells. *AIDS* **24**, 1107–1119 (2010).
40. Yadav, A. *et al.* HIVAN phenotype: consequence of epithelial mesenchymal transdifferentiation. *Am. J. Physiol. Renal Physiol.* **298**, F734–F744 (2009).
41. Ross, M.J. *et al.* Role of ubiquitin-like protein FAT10 in epithelial apoptosis in renal disease. *J. Am. Soc. Nephrol.* **17**, 996–1004 (2006).
42. Docherty, N.G., O'Sullivan, O.E., Healy, D.A., Fitzpatrick, J.M. & Watson, R.W. Evidence that inhibition of tubular cell apoptosis protects against renal damage and development of fibrosis following ureteric obstruction. *Am. J. Physiol. Renal Physiol.* **290**, F4–F13 (2006).
43. Zeisberg, M. & Kalluri, R. The role of epithelial-to-mesenchymal transition in renal fibrosis. *J. Mol. Med.* **82**, 175–181 (2004).
44. Quaggin, S.E. & Kapus, A. Scar wars: mapping the fate of epithelial-mesenchymal-myofibroblast transition. *Kidney Int.* **80**, 41–50 (2011).
45. Hertig, A., Flier, S.N. & Kalluri, R. Contribution of epithelial plasticity to renal transplantation-associated fibrosis. *Transplant. Proc.* **42**, S7–S12 (2010).
46. Mainra, R., Gallo, K. & Moist, L. Effect of N-acetylcysteine on renal function in patients with chronic kidney disease. *Nephrology (Carlton)* **12**, 510–513 (2007).
47. Di Stefano, V., Blandino, G., Sacchi, A., Soddu, S. & D'Orazi, G. HIPK2 neutralizes MDM2 inhibition rescuing p53 transcriptional activity and apoptotic function. *Oncogene* **23**, 5185–5192 (2004).
48. Rinaldo, C., Prodosmo, A., Siepi, F. & Soddu, S. HIPK2: a multitalented partner for transcription factors in DNA damage response and development. *Biochem. Cell Biol.* **85**, 411–418 (2007).

ONLINE METHODS

Cells. HEK293 and HK2 cells were obtained from American Type Culture Collection[49]. Primary human renal epithelial cells were obtained from PromoCell. Conditionally immortalized mouse podocytes were cultured as described[50]. Primary renal tubular epithelial cells were isolated from mouse kidneys as described in the **Supplementary Methods**.

Gene delivery. For HIV infection, pNL4–3:ΔG/P-EGFP, a *gag/pol*-deleted HIV-1 construct that contains EGFP in the *gag* open reading frame, and pHR′-IRES-EGFP, a control EGFP construct, were used to generate the VSV-G pseudotyped virus[51]. Lonza Nucleofector Technology (Basic Neucleofector kit for Primary Mammalian Epithelial Cells, Program T20) was used for the transfection of renal epithelial cells. For the *in vitro* experiments, cells were infected with HIV pseudotyped virus or control virus for 2 d and then transfected with expression constructs (WT-HIPK2, KD-HIPK2 or siRNAs) for 3 additional d. For the experiments in which the cells were treated with TGF-β, cells were transfected with expression constructs or siRNAs 3 d before treatment with TGF-β for 48 h.

Constructs and siRNAs. siRNA for SIAH1 (QIAGEN, FlexiTube siRNA SI03037839) and HIPK2 were purchased from Thermo Scientific (Dharmacon ON-TARGET siRNA). Negative Control siRNAs were used as negative experimental controls. The WT-HIPK2 and KD-HIPK2 constructs were obtained from R.H. Goodman, Oregon Health and Science University, Portland[52]. The SIAH1 expression vector was purchased from Open Biosystems. Lentivectors encoding for fusion proteins of mCherry with HIPK2 (WT-HIPK2 and KD-HIPK2) were generated as described in the **Supplementary Methods**.

Apoptosis analysis. An Annexin V-FITC Apoptosis Detection Kit (BD Bioscience), a FACSCalibur Flow cytometer (BD Biosciences) and CellQuest software (BD Biosciences) were used. Caspase 3 activity was measured using a Human Active Caspase-3 Immunoassay kit from R&D Systems.

Real-time PCR. Quantitative real-time PCR was performed using QIAGEN QuantiTect One Step RT-PCR SYBR green kit (QIAGEN). Data were analyzed using the $2^{-\Delta\Delta CT}$ method and are presented as fold changes relative to a control sample after normalization against the expression of housekeeping genes.

Western blot. Western blot was performed as described in the **Supplementary Methods**. The following antibodies were used: antibody to mouse HIPK2 (Santa Cruz), human HIPK2 (Abcam), SIAH1 (Novus), phosphorylated or total Smad3, p53, p65, LEF, vimentin, Snail, E-Cadherin, ZO-1 and TCF (Cell Signaling Technology), FSP-1 (Milipore), nephrin (a gift from L. Holzman), synaptopodin (a gift from P. Mundel) and β-actin and GAPDH (Sigma).

Immunostaining of cells and tissue. The immunostaining of cells and tissue are described in the **Supplementary Methods**. Archival human kidney biopsies were collected at Columbia University under a protocol approved by its Institutional Review Board.

HIPK2 kinase activity assay. HIPK2 activity was measured in nuclear protein extracts following a protocol provided by Millipore (**Supplementary Methods**).

NF-κB reporter assay. The NF-κB reporter assay was performed as described in the **Supplementary Methods**.

Mouse studies. The Institutional Animal Care and Use Committee committee of Mount Sinai School of Medicine approved all mouse studies. *Hipk2*$^{-/-}$ (knockout) mice were obtained from E. Huang[53]. Knockout mice were backcrossed to FVB/N mice for nine generations and then crossed to Tg26 mice to generate *HIPK2*$^{+/-}$; Tg26 mice. Subsequent crossings of *HIPK2*$^{+/-}$; Tg26 to *HIPK2*$^{+/-}$; Tg26 mice generated *HIPK2*$^{-/-}$; Tg26 (KO-Tg26), *HIPK2*$^{+/-}$; Tg26, *HIPK*$^{+/+}$; Tg26 (Tg26) mice and the corresponding non-Tg26 littermates. UUO-induced and folic acid–induced acute kidney injury models were created as described in the **Supplementary Methods**. Tg26 mice and their age- and sex-matched control littermates were fed NAC at 300 mg per kg of body weight or vehicle as described[54] by daily gavage. Mice of either sex were used unless otherwise specified.

Kidney histology. Histologic analyses of periodic acid-Schiff–stained slides were scored for the glomerulosclerosis index, podocyte hypertrophy and hyperplasia, as well as tubulointerstitial changes, as described[55]. Masson Trichrome and picrosirius red staining were performed to assess fibrosis[56]. Renal cortical collagen content was determined by morphometric measurement of areas stained with picrosirius red[57].

Affymetrix and Panomics protein and DNA arrays. Protein and DNA arrays (Combo Array, Affymetrix) were performed using nuclear proteins of kidneys from Tg26 and WT mice ($n = 5$) following the manufacturer's protocol. Data were analyzed as described in the **Supplementary Methods**.

Microarray studies. Affymatrix gene expression microarrays were performed at the Mount Sinai Institution Microarray Core Facility and analyzed as described in the **Supplementary Methods**.

Quantitative determination of tissue hydroxyproline. The hydroxyproline content in the kidney hydrolysates was quantified as described[58] and expressed as mg per mg of dry kidney weight.

Measurement of the glutathione to glutathione disulfide ratio. The glutathione to glutathione disulfide ratio was measured as described in the **Supplementary Methods**.

The isolation of glomeruli from mice for western blot and real-time PCR was performed as described[59,60]. The purity of the glomerular isolate was verified by microscopy and western blotting for synaptopodin, nephrin and Wilms tumor 1 (WT1).

Statistical analyses. All data are expressed as mean ± s.d. An unpaired *t* test was used to analyze data between two groups after determination of the data distribution. One-way ANOVA followed by either Bonferroni or Tukey multiple comparison tests was used when more than two groups were present to calculate significance. Statistical significance was considered when $P < 0.05$.

Computational network analysis. The promoter analysis was conducted by using TRANSFAC and ChEA. Protein interaction subnetworks were created using Gene2Networks. Kinase enrichment analysis was conducted using KEA. For details, see the **Supplementary Methods**.

49. Rosenstiel, P.E. *et al.* HIV-1 Vpr inhibits cytokinesis in human proximal tubule cells. *Kidney Int.* **74**, 1049–1058 (2008).
50. He, J.C. *et al.* Nef stimulates proliferation of glomerular podocytes through activation of Src-dependent Stat3 and MAPK1,2 pathways. *J. Clin. Invest.* **114**, 643–651 (2004).
51. Ross, M.J. *et al.* Role of ubiquitin-like protein FAT10 in epithelial apoptosis in renal disease. *J. Am. Soc. Nephrol.* **17**, 996–1004 (2006).
52. Zhang, Q., Yoshimatsu, Y., Hildebrand, J., Frisch, S.M. & Goodman, R.H. Homeodomain interacting protein kinase 2 promotes apoptosis by downregulating the transcriptional corepressor CtBP. *Cell* **115**, 177–186 (2003).
53. Winter, M. *et al.* Control of HIPK2 stability by ubiquitin ligase Siah-1 and checkpoint kinases ATM and ATR. *Nat. Cell Biol.* **10**, 812–824 (2008).
54. Ivanovski, O. *et al.* The antioxidant N-acetylcysteine prevents accelerated atherosclerosis in uremic apolipoprotein E knockout mice. *Kidney Int.* **67**, l2288–2294 (2005).
55. D'Agati, V. Pathologic classification of focal segmental glomerulosclerosis. *Semin. Nephrol.* **23**, 117–134 (2003).
56. He, W. *et al.* Wnt/beta-catenin signaling promotes renal interstitial fibrosis. *J. Am. Soc. Nephrol.* **20**, 765–776 (2009).
57. Junqueira, L.C., Bignolas, G. & Brentani, R.R. Picrosirius staining plus polarization microscopy, a specific method for collagen detection in tissue sections. *Histochem. J.* **11**, 447–455 (1979).
58. Yang, J., Dai, C. & Liu, Y. Hepatocyte growth factor gene therapy and angiotensin II blockade synergistically attenuate renal interstitial fibrosis in mice. *J. Am. Soc. Nephrol.* **13**, 2464–2477 (2002).
59. Takemoto, M. *et al.* A new method for large scale isolation of kidney glomeruli from mice. *Am. J. Pathol.* **161**, 799–805 (2002).
60. Ratnam, K.K. *et al.* Role of the retinoic acid receptor-alpha in HIV-associated nephropathy. *Kidney Int.* **79**, 624–634 (2011).